ELSEVIER

Journal of Food Engineering 64 (2004) 445–453

JOURNAL OF FOOD ENGINEERING

www.elsevier.com/locate/jfoodeng

Comparison of temperature distribution in model food cylinders based on Maxwell's equations and Lambert's law during pulsed microwave heating

H.W. Yang, S. Gunasekaran *

Food and Bioprocess Engineering Laboratory, Department of Biological Systems Engineering, University of Wisconsin-Madison, Agricultural Engineering Building 220, 460 Henry Mall, Madison, WI 53706, USA

Received 3 April 2002; received in revised form 7 July 2003; accepted 12 August 2003

Abstract

Two-percent agar gel cylinders were heated using pulsed and continuous microwave energy. Temperature distribution inside the sample was measured and compared with numerical predictions based on the Lambert's law and Maxwell's equations. The Maxwell's equations account for the standing wave effect inside the sample, the Lambert's law does not. The results show that the predictions based on the Maxwell's equations are statistically more accurate than those based on the Lambert's law, especially around the sample edge. The measured temperature distributions and the corresponding predictions using both models indicate better temperature uniformity in the agar gel cylinders under pulsed microwave heating, though the total process time is longer, than under continuous microwave heating.

Keywords: Pulsed microwave heating; Finite-difference model; Lambert's law; Maxwell's equation; Temperature distribution

1. Introduction

Heating food materials by electromagnetic radiation is widely used in commercial, industrial, and household applications. These applications rely on internal heat generated from interaction between the material and electromagnetic radiation. The propagation fields based on Maxwell's equations are associated with power flux, namely, Poynting vector of harmonic fields (Ayappa, Davis, Crapiste, Davis, & Gordon, 1991; Cheng, 1992).

The models developed based on oscillating power principle are useful for prediction of hot spots (Fu & Metaxas, 1992). The oscillating power absorption principle for thin slabs of food with differing dielectric properties is the key to number of patents by a group at Pillsbury Corp., Minneapolis, MN (Atwell, Pesheck, Krawjecki, & Anderson, 1990, 1992; Pesheck, Atwell, Krawjecki, & Anderson, 1991a, 1991b, 1992). These patents describe the principle that, by changing the thickness and thermal mass (product of sample mass and its specific heat capacity) of a given food layer the heating rate of that layer is changed.

In spheres and cylinders, a concentrated heating frequently occurs at the focal points within a sample (Ohlsson & Risman, 1978). Pangrle, Ayappa, Davis, Davis, and Gordan (1991) proposed models for cylindrical shapes to study phase changes of frozen brine (salted water) thawed by microwave energy. Yang and Gunasekaran (2001) studied the effect of pulsed microwave heating based on the Lambert's law to describe the electric field behavior in 2% agar gel cylinders. However, the Lambert's law does not account for node/anti-node formation (Barringer, Davis, Gordon, Ayappa, & Davis, 1995).

In the present study, Maxwell's equations, related to space and time dependence, were solved to determine the absorbed microwave power. The absorbed power was applied intermittently to a finite-difference heat transfer model to simulate the temperature distribution in 2% agar gel cylinders heated by pulsed microwave power.

* Corresponding author. Tel.: +1-608-262-1019; fax: +1-608-262-1228.

E-mail address: guna@facstaff.wisc.edu (S. Gunasekaran).

0260-8774/$ - see front matter © 2003 Published by Elsevier Ltd.
doi:10.1016/j.jfoodeng.2003.08.016

The objectives of this research were to:

- investigate the temperature distribution (TD) in 2% agar gel sample cylinders heated by continuous and pulsed microwave energy,
- predict the sample TD by solving the Lambert's Law and Maxwell's equations of microwave power absorbed by the samples,
- compare the measured and predicted TD in the sample under continuous and pulsed microwave heating.

2. Theory and analyses

2.1. Implicit finite-difference model

For a cylinder, the unsteady state (transient) differential equation can be solved term-by-term difference approximation of the equation:

$$\frac{\partial^2 T}{\partial r^2}+\frac{1}{r}\frac{\partial T}{\partial r}+\frac{\partial^2 T}{\partial z^2}+\frac{P}{k}=\frac{\partial T}{\alpha_H \partial t} \tag{1}$$

where T = sample temperature (°C), r = radial distance (m), z = axial distance (m), P = absorbed power (W), k = thermal conductivity ($W\,m^{-1}\,°C^{-1}$), t = time, and α_H = thermal diffusivity ($m^2\,s^{-1}$), respectively.

In the case of one-dimensional heat transfer, the third term of Eq. (1) on the left drops out. For the cylindrical geometry in finite-difference (FD) formulation, a typical inner node follows the first law of thermodynamics and yields:

$$\frac{V_i \rho C_p \mathrm{d}T_i}{\mathrm{d}t}=q_{i-1}\left(R_i-\frac{\mathrm{d}R}{2}\right)2\pi Z+q_{i+1}\left(R_i+\frac{\mathrm{d}R}{2}\right)2\pi Z+P_i \tag{2}$$

where R_i = distance from the sample center (m), V_i = volume between $R_i \pm \mathrm{d}R/2$ (m^3), P_i = power generation in V_i (W), ρ = density of the material (kg/m^3), C_p = specific heat capacity ($kJ\,kg^{-1}\,°C^{-1}$), $\mathrm{d}t$ = time increment (s) and $\mathrm{d}T_i$ = temperature difference at nodal point i between present time (t) and new time step ($t+\Delta t$) (°C). The heat flux terms, q_{i-1} and q_{i+1}, are related to temperature by the Fourier's law of conduction.

For a typical boundary nodal point, the second term on the right side in Eq. (2) is substituted by the convection boundary condition: $hA_s\ (T_i - T_{air})$, where, h = average heat transfer coefficient, A_s = surface area at the boundary (m^2) and T_{air} = temperature of ambient air (°C). The initial condition is: $T(t=0)=T_{intial}$ for $0 \leqslant r \leqslant R$. We have previously reported (Yang & Gunasekaran, 2001) the stability and the validation of this heat transfer model. The absorbed microwave power is obtained by solving the Lambert's law or Maxwell's equations.

2.2. The Lambert's law

The average temperature rise in a material during microwave heating time t depends on the total microwave energy absorbed by the material. The energy balance gives:

$$\Delta T_{av}=\frac{tP_{abs}}{V\rho C_p} \tag{3}$$

where, ΔT_{av} = average temperature rise (°C), P_{abs} = total power absorbed (W), t = heating time (s) and V = sample volume (m^3), ρ = sample density kg/m^3, C_p = sample specific heat capacity ($kJ\,kg^{-1}\,°C^{-1}$).

If one-dimensional analysis is considered and the incident radiation is assumed to be normal to the surface, the power dissipated at a certain sample depth is given by the exponential decay of the incident power along that direction (Fig. 1). The power term was derived by Von Hippel (1954) and is often referred to as the Lambert's law:

$$P(x)=P_0 e^{-2\beta x} \tag{4}$$

where, x = depth or distance from surface along the radial axis (m), $P(x)$ = power dissipated at the depth x

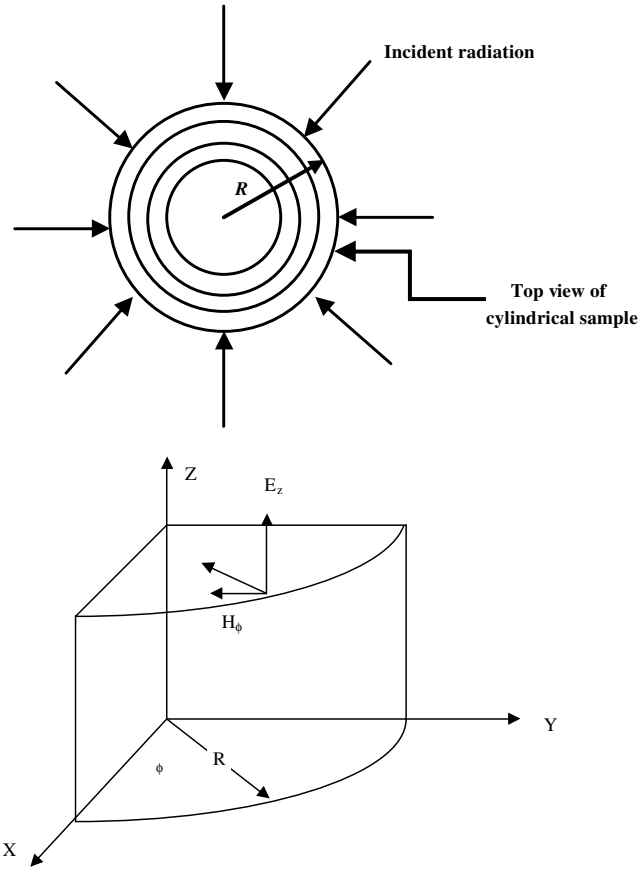

Fig. 1. Cylindrical coordinate system and corresponding unit vectors for the case of electromagnetic radiation incident normal to the surface.

(W), P_o = incident power or power at the surface (W), and β = attenuation constant (m^{-1}) which is a function of frequency of radiation, f (Hz); velocity of radiation, c (m/s); dielectric constant, κ'; and loss tangent, $\tan\delta$. It is given by the following equation:

$$\beta = \frac{2\pi f}{c}\sqrt{\frac{\kappa'\sqrt{1+(\tan\delta)^2}-1}{2}} \tag{4a}$$

To calculate the incident power (P_o), the total absorbed power (P_{abs}) is expressed as the volume integral of the $P(x)$ function. For a cylindrical sample in an azimuthal wave field:

$$P_{abs} = \int_v P(x)\,dV = \int_0^Z\int_0^{2\pi}\int_0^R P_o e^{-2\beta x}\,dx\,du\,dz \tag{5}$$

where, Z and R are the height and radius of the test sample (m), respectively. The power absorbed by each cylindrical shell (P_i) in the sample based on the Lambert's law is (Padua, 1993; Yang & Gunasekaran, 2001):

$$\begin{aligned} P_i &= \int_0^Z\int_0^{2\pi}\int_{x_2}^{x_1} P_0 e^{-2\beta x}\,dx\,du\,dz \\ &= \frac{\pi Z P_0}{\beta}\left(e^{-2\beta x_1}-e^{-2\beta x_2}\right) \end{aligned} \tag{6}$$

where the subscripts 1 and 2 refer to the outer and inner peripheries of the shell. In the case of pulsed microwave application, the power term for each node (P_i) is applied to Eq. (2).

2.3. Maxwell's power dissipation

A propagating electromagnetic wave is composed of oscillating electric (***E***) and magnetic (***B***) field components. Maxwell's equations describing their space and time variations are:

$$\nabla\times E = -\frac{\partial B}{\partial t} \quad \text{and} \quad \nabla\times H = J + \frac{\partial D}{\partial t} \tag{7}$$

where ***E*** ($V\,m^{-1}$) and ***H*** ($A\,m^{-1}$) are the electric and magnetic fields, ***J*** = current flux ($A\,m^{-2}$), D = electric displacement ($C\,m^{-2}$) and B = magnetic induction ($Wb\,m^{-2}$). With the help of (i) constitutive relations using the time dependence expression, (ii) material magnetic permeability μ approximated by its value in free space, (iii) electroneutral condition of the material and (iv) one-dimensional azimuthal microwave behavior in a cylinder, Maxwell's equations yield:

$$\frac{d^2E}{dr^2} + \frac{1}{r}\frac{dE}{dr} + k_1^2 E = 0 \quad \text{for } 0 \leqslant r \leqslant R \tag{8}$$

where $k_1^2 = \omega^2\mu_0\varepsilon_0(\kappa' + i\kappa'')$, ω = angular velocity ($rad\,s^{-1}$), μ_0 = free space permeability ($H\,m^{-1}$), ε_0 = free space permittivity ($F\,m^{-1}$), κ' = dielectric constant and κ'' = dielectric loss factor.

Eq. (8) is rendered dimensionless by substituting:

$$r^* = \frac{r}{R} \quad \text{and} \quad u = \frac{E}{E_0} \tag{9}$$

Noting that $u = v + iw$, Eq. (7) reduces to the following two equations that are solved with their appropriate boundary conditions:

$$\frac{d^2v}{dr^{*2}} + \frac{1}{r^*}\frac{dv}{dr^*} + \psi v - \chi w = 0 \tag{10}$$

and

$$\frac{d^2w}{dr^{*2}} + \frac{1}{r^*}\frac{dw}{dr^*} + \psi w + \chi v = 0 \tag{11}$$

where $\psi = R^2\omega^2\mu_0\varepsilon_0\kappa'$, $\chi = R^2\omega^2\mu_0\varepsilon_0\kappa''$. The boundary conditions at $r^* = 0$ are:

$$\frac{dv}{dr^*} = \frac{dw}{dr^*} = 0 \tag{12}$$

while boundary conditions at $r^* = 1$ are:

$$\frac{dv}{dr^*} + c_1 v + c_2 w = c_3 \tag{13}$$

and

$$\frac{dw}{dr^*} + c_1 w - c_2 v = c_4 \tag{14}$$

where

$$c_1 = R\alpha_0\left[\frac{J_1(\alpha_0R)J_0(\alpha_0R) + Y_1(\alpha_0R)Y_0(\alpha_0R)}{J_0^2(\alpha_0R) + Y_0^2(\alpha_0R)}\right],$$

$$c_2 = \frac{2}{\pi[J_0^2(\alpha_0R) + Y_0^2(\alpha_0R)]}$$

$$c_3 = -\frac{4}{\pi}\frac{Y_0(\alpha_0R)}{J_0^2(\alpha_0R) + Y_0^2(\alpha_0R)};$$

$$c_4 = -\frac{4}{\pi}\frac{J_0(\alpha_0R)}{J_0^2(\alpha_0R) + Y_0^2(\alpha_0R)}$$

where J and Y are Bessel functions, subscripts 0 and 1 are zero-order and first-order of Bessel functions and α_0 = is the free space wave number (m^{-1}), E_0 ($V\,m^{-1}$) is the intensity of the incident field related to power term P_0 (W) by:

$$P_0 = \frac{c\varepsilon_0 E_0^2}{\pi\alpha_0 R} \tag{15}$$

The power term as a function of r^* is calculated from v and w based on the Poynting vector:

$$P(r^*, t) = R^2\omega\varepsilon_0\kappa'' E_0(v^2 + w^2) \quad \text{for } 0 \leqslant R^* \leqslant 1 \tag{16}$$

For the case of constant properties, the coupled Eqs. (13) and (14) can be solved with the help of (Yang, 2002):

$$C_1 = \frac{c_3 + ic_4}{-(C_2 + iC_3)J_1(C_2 + iC_3) + (c_1 + ic_2)J_0(C_2 + iC_3)}$$

where $C_2 + iC_3 = \sqrt{\psi + i\chi}$. (17)

Table 1
Dielectric, physical, and thermal properties of 2% agar gel

Property	Value
Specific heat capacity, C_p (kJ/kg.°C)	4.2[a]
Thermal conductivity, k (W/m.°C)	0.60[a]
Density, ρ (kg/m^3)	1070[a]
Dielectric constant, κ'	73.6[a]
Dielectric loss, κ''	11.5[a]
Average surface heat transfer coefficient (h)	41.7[b]

[a] Data from Barringer et al. (1995).
[b] Data from Yang and Gunasekaran (2001).

The analytical solutions of the coupled equations are:

$$v(r^*) = \mathrm{Re}\{C_1 J_0[(C_1 + \mathrm{i}C_2)r^*]\} \quad (18)$$

$$w(r^*) = \mathrm{Im}\{C_1 J_0[(C_1 + \mathrm{i}C_2)r^*]\} \quad (19)$$

where Re and Im refer to corresponding real and imaginary parts.

2.4. Temperature distribution prediction

Applying the two forms of microwave power solutions based on the Lambert's law or Maxwell's equations to the implicit finite-difference heat transfer model, the interior temperature profile of a microwave-heated sample can be predicted. For pulsed microwave heating the absorbed power is zero in the heat transfer equation during the power-off periods. The software used for computation is MATLAB (MathWorks Inc., Natick, MA). The physical and thermal properties (Table 1) of agar gel reported by Barringer et al. (1995) were used in the calculations, though we recognize that material properties change during microwave heating.

3. Methods and materials

3.1. Microwave oven

A laboratory microwave oven (Labotron 500, Zwag Inc., Epone, France) operating at 2.45 GHz and output power setting of 250 W was used. The $33 \times 22 \times 35$-cm (width × height × depth) oven cavity houses a 25×3.5 cm (diameter × height) turntable that rotates at 15 rpm. The velocity of the outlet air, measured using a vane anemometer (Keuffel and Esser Co. New York), during microwave oven operation was 0.84 m/s.

3.2. Sample preparation

Agar gel samples were prepared by dissolving 40 g (2%) of agar powder (Bacto Agar, Difco Inc., Detroit, MI) in 1960 mL of warm (~40 °C) distilled water in a 2000-mL pyrex glass beaker. The agar-water solution was heated until agar powder was totally dissolved and the gel solution was clear. It was then poured into 600-mL or 400-mL pyrex glass beakers and cooled to room temperature into solid sample cylinders. The radii of samples prepared in 600-mL and 400-mL beakers were 4 cm and 3.5 cm, respectively. The sample height in both cases was 7 cm. The sample cylinders were stored at 4 °C for 16 h to ensure uniform initial sample temperature for microwave heating. The plastic film wrap (Saran Warp, The Dow Chemical Company, Indianapolis, IN) was used to cover the beakers during the heating, cooling and storing to prevent moisture loss.

3.3. Microwave process

The microwave oven was operated at pulsing ratios (duty cycles) of 1 (continuous), 2 (30-s power-on, 30-s power-off) and 3 (20-s power-on, 40-s power-off). The pulsing ratio, PR, is defined as:

$$\mathrm{PR} = \frac{(t_{\mathrm{on}} + t_{\mathrm{off}})}{t_{\mathrm{on}}} \quad (20)$$

where, t_{on} and t_{off} = duration of the microwave power-on and -off per duty cycle (s), respectively. The total microwave power-on time for all experiments was 3 min. However, it should be noted that the total process time for PR = 1,–3 are respectively 3, 6, and 9 min.

3.4. Temperature measurement

For each experiment, one agar gel cylinder was placed at the center of the turntable in the microwave oven. For every sample, temperatures were measured across the horizontal mid-plane (i.e., $z = 3.5$ cm) at the radial distances of 0–3 cm for 3.5-cm radius samples and 0–4 cm for 4-cm radius samples. The sample cylinder was removed from the microwave oven after every minute of microwave heating, and temperature measurements were made. A new sample was used for temperature measurements after each time interval. A type-T thermocouple probe (0.82-mm diameter) (Omega Engineering Inc., Stamford, CT) connected to a data-logger (Model 34970A, Hewlett Packard, Beverton, OR) was used to measure the temperature. The time constant of the thermocouple was about 0.25 s. A 0.5-cm thick cardboard with holes drilled 1 cm from each other along the radius was placed on top of the agar gel cylinder matching the sample edge. The thermocouple probe was then inserted into the sample via the holes in the cardboard until it reached the mid-plane. Single thermocouple was used for all measurements. The readings were taken starting from the sample center (0 cm) and moving outward. The temperature at each location was measured in triplicates using three samples. The average and the standard deviation of the three temperature measurements were calculated to represent the temperature distribution in the sample cylinder. For each sample, all temperature measurements were completed

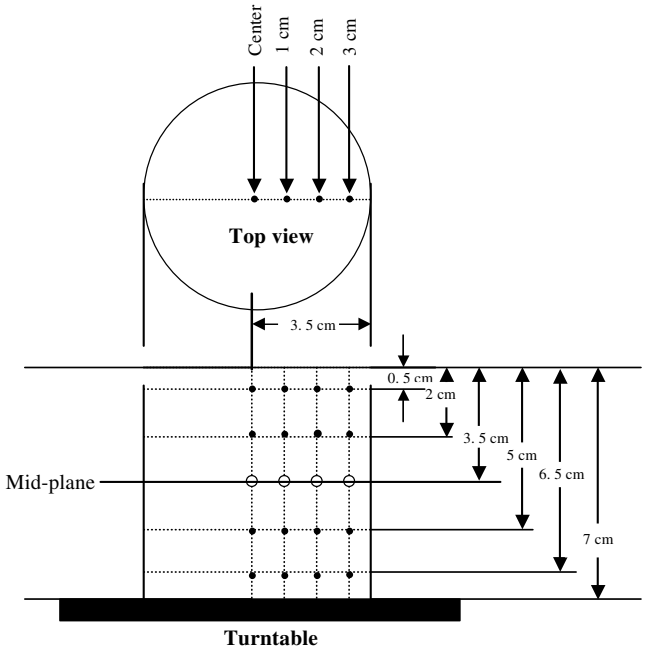

Fig. 2. Temperature measurement locations in 3.5×7 cm (radius× height) agar gel cylinders for validating one-dimensional heat transfer assumption.

within 30 s after the sample was removed from the microwave oven. The temperature variation at each location due to the 30-s delay during the measurements was determined. The effect of this 30-s delay (handling time effect) on temperature measurement was evaluated (Fig. 1)

The sample dimensions used raised a concern if they can satisfy one-dimensional radial heat transfer assumption To validate this temperatures were measured along the z-axis at different heights as shown in Fig. 2 at the microwave power setting of 250 W. We note here that Mudgett (1986) showed that one-dimensional model is satisfactory for his samples of similar dimensions (5-cm radius×7-cm height agar gel cylinders).

3.5. Average absorbed microwave power

The average absorbed power (P_{abs}) in the microwave oven was determined experimentally. The 250-W oven setting was employed to heat distilled water of different volumes (ranging from 56 to 352 cm^3) for 180 s (Yang, 2002). The efficiency of energy transfer between the microwave oven and the food sample is related to the product's dielectric properties. The efficiency is also related to the nature of the product and volumetric load of the sample (Mudgett, 1986). The average temperature rise (ΔT_{av}), the difference between the temperatures before and after microwave heating, was measured. The temperatures were measured after stirring the heated water for 10 s using a hand mixer (KitchenAid, KTM-7) at the lowest speed (250 rpm) to ensure temperature uniformity. The distilled water can be lost during the microwave heating due to the moisture evaporation. The effect of evaporative cooling was determined by measuring the difference in mass of distilled water (Δw) before and after microwave heating. The average temperature rise (ΔT_{av}) was calculated from the following energy balance relationship:

$$P_{abs} = \frac{\rho V C_p \Delta T_{av} + h_{fg} \Delta w}{t} \quad (21)$$

where, ρ = density of distilled water ($=1000\ kg\,m^{-3}$), V = volume of the distilled water, C_p = specific heat capacity ($=4.18\ kJ\,kg^{-1}\,°C^{-1}$), ΔT_{av} = average temperature rise (°C) and t = microwave heating period (180 s), h_{fg} = latent heat of water ($=2338$ kJ/kg at 27 °C and atmospheric pressure). Three replications of temperature rise measurements were made.

The variation in the absorbed microwave power as a function of sample placement on the turntable (at 0–2 cm away from the turntable center) was evaluated. The absorbed power and the power-absorption efficiency (ratio of absorbed power to microwave oven power setting during processing) in the microwave oven for both experimental conditions were determined.

3.6. Validation of azimuthal microwave heating assumption

The assumption of azimuthal microwave heating was also validated by measuring the sample temperatures at the same radial distance but at different angular locations (0°, 120° and 240°). Temperature variation along the z-axis in 3.5×7 and 4×7 cm (radius×height) agar gel cylinder after being heated in the microwave oven used was evaluated. The heating duration was 3 min at 250-W oven setting and the temperature distribution in the agar gel cylinders was measured. The measured points are shown in Fig. 2. The temperature distributions in the 3.5- and 4-cm diameter sample cylinder were determined.

The χ^2-test was used to accept or reject the hypothesis that measured and predicted temperatures were the same, at $P = 0.01$ (Bender, Douglass, & Kramer, 1981).

4. Results and discussion

The effect of the maximum 30-s delay during temperature measurement did not significantly ($P > 0.01$, *F-test*) affect the temperatures measured. The temperatures measured at 0 and 2 cm from center in 3.5-cm and 4-cm radius samples after 3 min of continuous heating at 250-W microwave oven power setting are shown in Fig. 3.

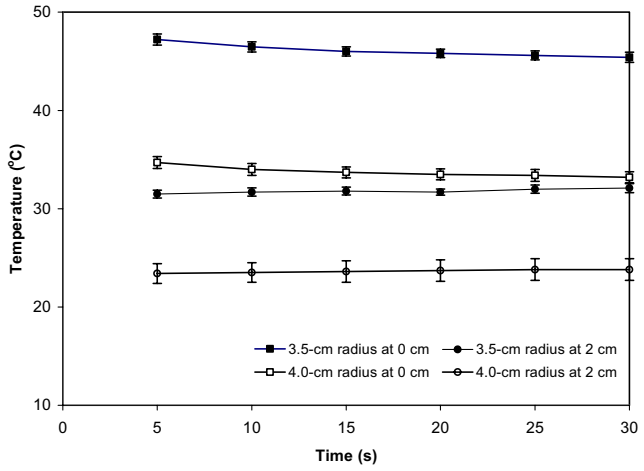

Fig. 3. Temperature variation at measurement locations 0 and 2 cm from center in 3.5- and 4-cm radius 2% agar gel cylinders during 30 s of handling after 3-min microwave heating. The vertical error bars are shown.

Table 3
Temperatures (mean ± standard deviation, °C) at different angular locations in a 3.5-cm agar gel cylinder

Location from center (cm)	Angular location		
	0°	120°	240°
0	14.9 ± 0.61	–	–
1	8.7 ± 0.17	8.4 ± 0.25	8.2 ± 0.1
2	10.5 ± 0.38	10.1 ± 0.35	10.3 ± 0.31
3	11.7 ± 0.40	12.6 ± 0.25	12.8 ± 0.40

Table 4
Paired *t*-test for temperatures at mid-plane (MP, $z = 3.5$ cm) compared to other locations along *z*-axis of agar gel samples

Depth (cm)	3.5-cm radius sample		4-cm radius sample	
	t-value	*P*	*t*-value	*P*
MP vs. average	1.24	0.323	1.42	0.229
MP vs. 0.5	2.37	0.098	3.83	0.019
MP vs. 2.0	1.20	0.455	3.60	0.023
MP vs. 5.0	2.46	0.091	1.62	0.181
MP vs. 6.5	5.17	0.014	3.87	0.018

The variation in microwave absorbed power as a function of sample placement (226 ± 3.7 W) on the turntable was also not statistically significant ($P > 0.01$). The absorbed power and the power-absorption efficiency in the microwave oven for both sample sizes are listed in Table 2. The power-absorption efficiency increased as the sample volume increased. The temperature variation at different spatial angles was not significant (Table 3). Each set of temperatures measured at the same horizontal plane along *z*-axis (Yang, 2002) was compared to that at the mid-plane (depth = 3.5 cm) using a paired *t-test*. The data presented in Table 4 indicate that the temperature set at all *z* locations are not significantly ($P > 0.01$) different from that at the mid-plane. Therefore, the mid-plane temperatures can represent the average temperature along the *z*-direction. This also validates out one-dimensional heat transfer assumption.

Maxwell's and Lambert's microwave power distribution in the 3.5- and 4-cm radius agar cylinders as a function of radius is shown in Fig. 4. The electric field was assumed to orient along the *z*-direction. The Maxwell's power distribution presents an oscillating pattern due to the space and time dependence of electromagnetic fields. The Lambert's power distribution presents an exponential decay function because the node/anti-node effect of waves is not considered. The Lambert's power

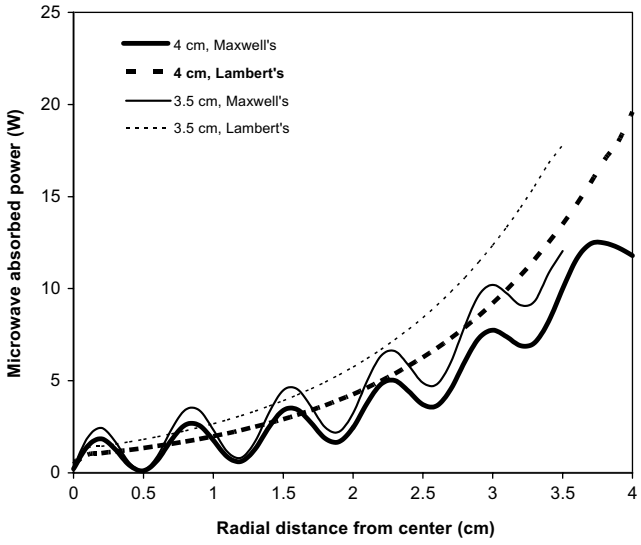

Fig. 4. Maxwell's and Lambert's model predicted microwave power absorbed during continuous heating of 2% agar gel cylinders (3.5- and 4-cm radius) as a function of radial distance from sample center. The electric field is oriented along the vertical *z*-axis of the cylinder.

at the outer portion of the sample along *r*-axis is significantly larger than the Maxwell's prediction. The power absorbed in the 3.5-cm radius sample cylinder is

Table 2
Absorbed power and energy-transfer efficiency in the microwave oven at 2.45 GHz and 250-W oven setting

Sample radius (cm)	Sample volume (cm^3)	Absorbed power (mean ± standard deviation, W)	Power-absorption efficiency (%)
3.5	269	223.5 ± 3.70	89.4
4.0	352	233.9 ± 2.89	93.6

generally larger than that in a 4-cm sample cylinder at the same radial distance. Theoretically, for smaller radius samples, the oscillating microwave power pattern is stronger because of the penetrating nature of the microwaves (Fu & Metaxas, 1992).

In the case of a cylindrical body, the annular incremental volume (V_i) along the r-axis converges as a function of $1/r^2$ from the sample surface to the center (same sample height, where r = radial distance). The absorbed microwave power (P_{abs}) generally decreases exponentially from the sample surface. Due to the combination effect of absorbed power and incremental volume, the power density (power absorbed per unit sample volume, P_{abs}/V_i) represents the focusing effect of microwave heating (Fig. 5) and the hot spot along the r-axis (i.e., sample center). The location of power focusing depends on the sample size, and is not necessarily at the center for a very large sample.

The measured and predicted sample temperature profiles at the end of 1 and 3 min heating by microwave power source with PR = 1–3 (continuous microwave power for PR = 1) for are shown as Figs. 6 and 7. For all the microwave processes, the largest temperature difference between any two consecutive measured points occurred at $R = 0$ and 1 cm. As the duration of microwave heating increased, the temperature difference inside the sample increased. The pulsed microwave heating resulted in lower temperature differences and minimized the hot spot effect.

For continuous microwave heating process, the sample temperature profiles predicted by the Maxwell's equations represent an oscillating pattern and agree with

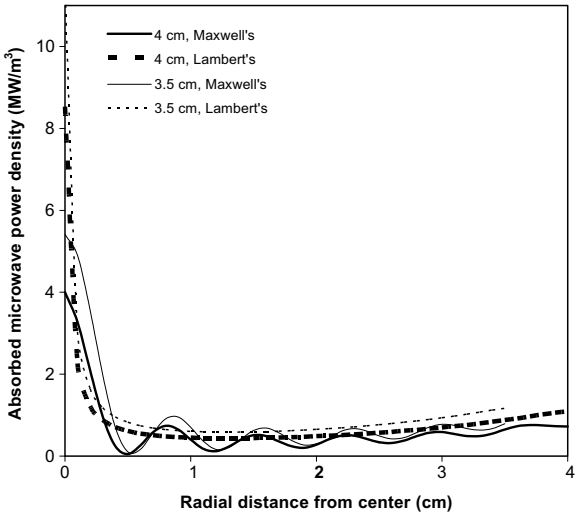

Fig. 5. Maxwell's and Lambert's model predicted microwave power density absorbed during continuous heating of 2% agar gel cylinders (3.5- and 4-cm radius) as a function of radial distance from sample center. The electric field is oriented along the vertical z-axis of the cylinder.

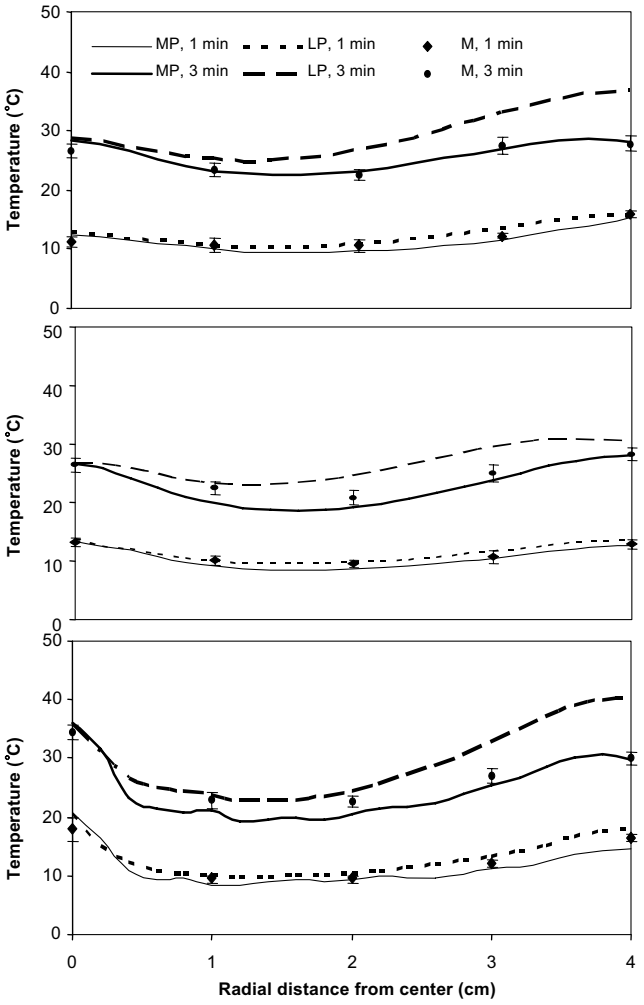

Fig. 6. Predicted temperature profiles based on Maxwell's (MP) and Lambert's (LP) models compared to the measured (M) temperature profile in 4-cm radius 2% agar gel cylinders after 1 and 3 min of microwave heating with pulsing ratio (PR) of 1–3 (symbols represent measured data along with error bars).

the power deposition. For pulsed microwave heating, the sample temperature profiles based on Maxwell's prediction represent fairly smooth curves. The results are as expected because during power-off periods of the pulsed microwave application, thermal diffusion helps to equalize the oscillating temperatures established during microwave power-on periods (Yang & Gunasekaran, 2001).

The measured temperatures were compared to the predicted temperatures based on Maxwell's equations and the Lambert's Law using the χ^2-test after 1–3-min of total microwave application (Table 5). The $\chi^2 = 45.6$ at $P = 0.01$ with degrees of freedom = 26 (Bender et al., 1981). The predicted TD based on either Maxwell's or Lambert's power is not significantly different from the measured TD ($P > 0.01$). However, the Lambert's prediction results in overestimating the temperature near

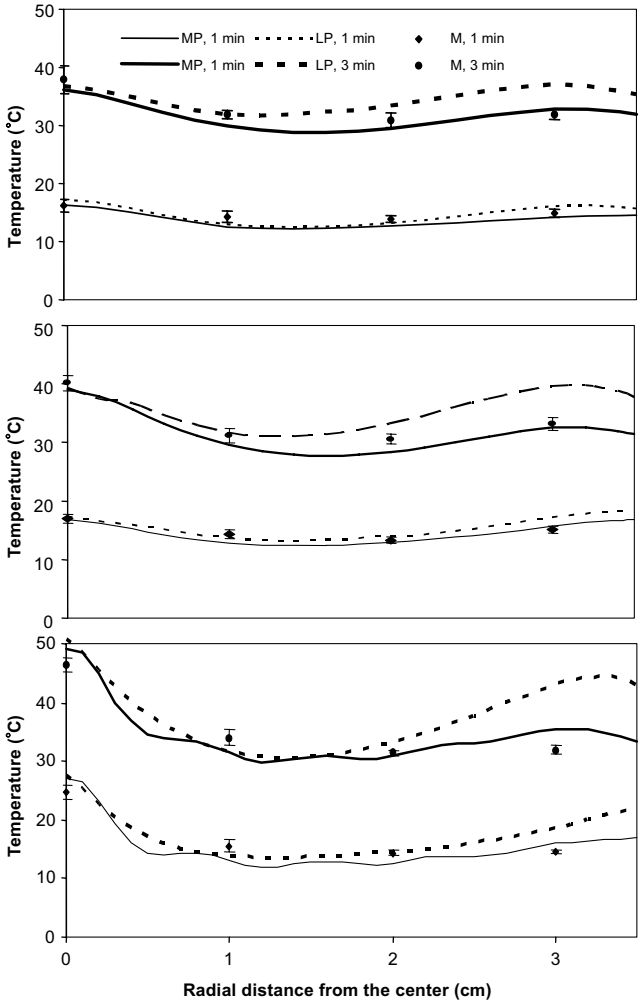

Fig. 7. Predicted temperature profiles based on Maxwell's (MP) and Lambert's (LP) models compared to the measured (M) temperature profile in 3.5-cm radius 2% agar gel cylinders after 1 and 3 min of microwave heating with pulsing ratio (PR) of 1–3 (symbols represent measured data along with error bars).

Table 5
Chi-square values for Maxwell's and the Lambert's predictions compared to the measured temperatures during microwave heating

Microwave processing time (min)	χ^2 of Maxwell's prediction	χ^2 of Lambert's prediction
1	5.56	7.25
2	3.86	10.01
3	4.24	16.06

the sample surface. The calculated χ^2 increased as microwave heating time increased for the Lambert's predictions but remained about the same for the Maxwell's predictions. These statistical results indicate that Maxwell's prediction is more accurate than the Lambert's for long heating times.

5. Conclusions

The predicted temperature profiles within the sample based on either the Lambert's law or Maxwell's equations were statistically accurate as compared to the measured temperatures. The power formulation based on Maxwell's equations is more accurate than that based on Lambert's, especially at the outer boundary of the sample. Due to the semi-infinite critical sample length assumption of the Lambert's law, the standing wave effect was not considered, the temperature at 3-cm for the 3.5-cm radius (smaller) sample thus was overestimated. The local hot spot observed at the sample center during continuous microwave heating is substantially reduced by pulsed microwave heating under the conditions of same total microwave heating time (total magnetron on-time). It should be noted, however, the pulsed microwave application takes longer total process time than continuous microwave application.

References

Atwell, W. A., Pesheck, P. S., Krawjecki, M. M., & Anderson, G. R. (1990). *Microwave food products and method of their manufacture*. US patent no. 4926020, US Patent and Trademark Office, Alexandria, VA.

Atwell, W. A., Pesheck, P. S., Krawjecki, M. M., & Anderson, G. R. (1992). *Microwave food products and method of their manufacture and heating*. US patent no. 5101084, US Patent and Trademark Office, Alexandria, VA.

Ayappa, K. G., Davis, H. T., Crapiste, G., Davis, E. A., & Gordon, J. (1991). Microwave heating an evaluation of power formulations. *Chemical Engineering Science, 46*, 1005–1016.

Barringer, S. A., Davis, E. A., Gordon, J., Ayappa, K. G., & Davis, H. T. (1995). Microwave-heating temperature profiles for thin slabs compared to Maxwell and Lambert law prediction. *Journal of Food Science, 60*, 1137–1142.

Bender, F. B., Douglass, L. W., & Kramer, A. (1981). *Statistical methods for food and agriculture*. Binghamton, New York: Food Products Press Inc.

Cheng, D. K. (1992). *Field and wave electromagnetics*. Reading, MA: Addison-Wesley Publishing Company.

Fu, W., & Metaxas, A. (1992). A mathematical derivation of power penetration depth for thin lossy materials. *Journal of Microwave Power, 27*, 217–222.

Hippel, A. R. (1954). *Von dielectrics and waves*. New York: Wiley.

Mudgett, R. E. (1986). Microwave properties and heating characteristics of foods. *Food Technology, 40*, 84–93.

Ohlsson, T., & Risman, P. O. (1978). Temperature distribution of microwave heating-spheres and cylinders. *Journal of Microwave Power, 13*, 303–309.

Padua, G. W. (1993). Microwave heating of agar gels containing sucrose. *Journal of Food Science, 58*, 1426–1428.

Pangrle, B. J., Ayappa, K. G., Davis, H. T., Davis, E. A., & Gordan, J. (1991). Microwave thawing of cylinders. *AIChE Journal, 37*, 1789–1800.

Pesheck, P. S., Atwell, W. A., Krawjecki, M. M., & Anderson, G. R. (1991a). *Microwave food products and method of their manufacture*. US patent no. 4988841, US Patent and Trademark Office, Alexandria, VA.

Pesheck, P. S., Atwell, W. A., Krawjecki, M. M., & Anderson, G. R. (1991b). *Microwave food products and method of their manufacture*. US patent no. 5008507, US Patent and Trademark Office, Alexandria, VA.

Pesheck, P. S., Atwell, W. A., Krawjecki, M. M., & Anderson, G. R. (1992). *Microwave food product and methods of their manufacture and heating*. US patent no. 5140121, US Patent and Trademark Office, Alexandria, VA.

Yang, H. W., & Gunasekaran, S. (2001). Temperature profiles in a cylindrical model food during pulsed microwave heating. *Journal of Food Science, 66*, 998–1004.

Yang, H. W. (2002). Analysis of temperature distribution in model foods during continuous and pulsed microwave heating. Ph.D. Thesis, University of Wisconsin-Madison.